

1

2 Investigation of the extreme wet-cold compound events changes between 2025-2049 and
3 1980-2004 using regional simulations in Greece

4 Iason Markantonis^{1,2}, Diamando Vlachogiannis¹, Athanasios Sfetsos¹, Ioannis Kioutsioukis²

5 ¹Environmental Research Laboratory, NCSR “Demokritos”, 15341 Agia Paraskevi, Greece

6 ²University of Patras, Department of Physics, University Campus 26504 Rio, Patras, Greece

7 *Correspondence to:* Iason Markantonis (jasonm@ipta.demokritos.gr)

8 **Abstract.** This paper aims to study wet-cold compound events (WCCEs) in Greece for the wet and
9 cold season November-April, since these events may affect directly human activities for short or longer
10 periods as no similar research has been conducted for the country studying the past and future
11 development of these compound events. WCCEs are divided into two different daily compound events
12 (Maximum Temperature (TX) -Accumulated Precipitation (RR)) and (Minimum Temperature (TN) –
13 Accumulated Precipitation (RR)) using fixed thresholds (RR over 20 mm/day and Temperature under 0
14 °C). Observational data from the Hellenic National Meteorology Service (HNMS) and simulation data
15 from reanalysis and EURO-CORDEX models were used in the study for the historical period 1980-
16 2004. The Ensemble mean of the simulation datasets from projection models ~~were~~ was employed for
17 the near future period (2025-2049) to study the impact of climate change on the occurrence of WCCEs
18 under the Representative Concentration Pathways (RCPs) 4.5 and 8.5 scenarios. Following data
19 processing and validation of the models, the potential changes in the distribution of WCCEs in the
20 future were investigated based on the projected and historical simulations. WCCEs determined by fixed
21 thresholds were mostly found over high altitudes with TN-RR events exhibiting a future tendency to
22 reduce particularly under the RCP 8.5 scenario and TX-RR exhibiting similar reduction of probabilities
23 for both scenarios.

24

25 1. Introduction

26 Extreme weather events and their linkage to climate change is a matter of high concern for many
27 scientific groups (Zanocco et al., 2018; Konisky et al., 2016; Curtis et al., 2017). In the last decade,
28 numerous scientific studies focused on the causes, ~~the~~ frequency and impacts of extreme compound
29 events (e.g. Aghakouchak et al., 2020; Singh et al., 2021; Sadegh et al., 2018; Zscheischler et al., 2017;
30 Zscheischler and Seneviratne, 2017; Zscheischler et al., 2018). As mentioned in the Intergovernmental
31 Panel on Climate Change report on “Managing the risks of extreme events and disasters to advance
32 climate change adaptation” (IPCC SREX) (Ref 7, p. 118) compound events are defined as: (1) two or
33 more extreme events occurring simultaneously or successively, (2) combinations of extreme events
34 with underlying conditions that amplify the impact of the events, or (3) combination of events that are
35 not themselves extremes but lead to an extreme event or impact when combined (Leonard et al., 2014).

36 Recent studies have been conducted on the examination of wet-cold compound events (WCCEs) that
37 concern daily values of temperature and precipitation and the correlation of these variables
38 (Chukwudum and Nadarajah, 2022; Lhotka and Kyselý, 2021)—, while other studies focus on the
39 occurrence of monthly WCCEs for the historical period (Wu et al., 2019; Lemus-Canovas, 2022)
40 However, the purpose of this article is the study of fixed thresholds extreme WCCEs on daily basis in
41 Greece during the historical period (1980-2004) and how the likelihood of these events will be affected
42 by climate change, during the period 2025-2049. It has been reported that WCCEs affect the region of
43 the Mediterranean Basin, including Greece (Zhang et al., 2021). Studies using only observational data
44 at some locations (Lazoglou and Anagnostopoulou, 2019), or modeled data mostly over the broader
45 region of the Mediterranean Sea (Vogel et al., 2021; Hochman et al., 2021; de Luca et al., 2020),
46 concerning WCCEs have been conducted in the past, but not depicting analytically WCCEs in Greece,
47 a country that as a part of the Mediterranean Basin is considered a “Climate change hotspot” (Ali et al.,
48 2022;-). This work attempts to fill this void on the effects of climate change on WCCEs in Greece.

49 The examined events belong to the first category of the definition of compound events from IPCC
50 since they refer to the simultaneous exceedance of precipitation and temperature thresholds. WCCEs
51 may have a negative impact on people's lives by causing electricity blackouts, affecting agriculture
52 with heavy snowfall or freezing rain and blocking transportation because of closed roads, railways or
53 even airports (Houston et al., 2006; Llasat et al., 2014; Vajda et al., 2014). On the other hand, most of
54 the available freshwater in the country comes from melted mountain snow during spring or summer.
55 Finally, eco-systems, especially in mountains, may be affected by the absence of snow that climate
56 change may cause (Demiroglu et al., 2015; Pestereva et al., 2012; Trujillo et al., 2012; García-Ruiz et
57 al., 2011).

58 The first part of the study concerns the historical period between 1980 and 2004, because of the
59 availability of quality-controlled daily observational data for minimum temperature (TN), maximum
60 temperature (TX) and accumulated precipitation (RR). Hence, for that period, we use observational
61 data from 21 Hellenic National Meteorological Service (HNMS) stations, to validate EURO-CORDEX
62 Regional Climate Models (RCMs), provided by the Copernicus Climate Change Service and the
63 projection model dataset produced in-house. In addition to the models, two reanalysis products are
64 included, as the closest to "true" past climate conditions in regions with no or scarce observations
65 (Moalafhi et al., 2016). More information about the observational and model datasets is presented in
66 Section 2. Section 3 highlights the applied methodology while Section 4 displays WCCEs observed in
67 stations and station cells of the models and Section 5 ~~contains-discusses the~~ reanalysis and projections
68 Ensemble mean WCCEs probabilities spatial distribution for the historical period. Section 6 details the
69 results ~~about~~ of the difference in WCCEs probabilities between the historical and the near future period
70 between 2025 and 2049 for two greenhouse gas concentration scenarios, RCP 4.5 and RCP 8.5.

71 2. Data

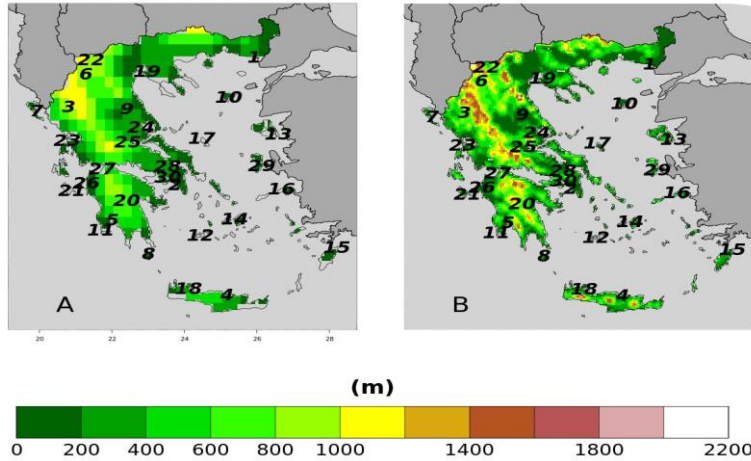
72 In this Section, we present the datasets that provide the observational and simulation data produced by
73 projection and reanalysis models.

74 2.1. HNMS observations

75 HNMS provides freely observational data from 21 stations for the purpose of scientific research
76 (<http://www.emy.gr/emv/el/services/paroxi-ipiresion-elefthera-dedomena>). The data have been
77 formally evaluated by HNMS and the timeseries show no missing or distorted values. In particular, the
78 timeseries available for the historical period 1980-2004 have a 3-hour temporal resolution and from
79 these values, we have extracted the daily values of TN, TX and RR. Moreover, stations 22-30 ~~that~~
80 ~~which~~ also belong ~~in-to~~ the network of HNMS stations contain observations in the period 1980-2004,
81 although none of the stations covers all observational days in the period. The datasets of these stations
82 were extracted by the National Centers for Environmental Information of National Oceanic and
83 Atmospheric Administration. We selected stations that contain at least 20 years of observations. Figure
84 1 shows the position of the stations on the orography of ~~-~~ERA5 and WRF, while Table A1 of the
85 Appendix- provides details on the characteristics of the stations. We have used ~~the~~ observational data to
86 validate the model datasets regarding the WCCEs for the historical period.

87

Μορφοποιήθηκε: Χωρίς κουκκίδες ή αρίθμηση



88

89 **Figure 1: Map of HNMS stations on orography of (A) ERA5 and (B) WRF-ERAinterim. The**
 90 **numbers correspond to those in Table A1 (Appendix).**

91 **2.2. Reanalysis models**

92 We have used two reanalysis models due to the lack of spatially and temporally complete direct
 93 observations, to study more consistently the WCCes in Greece in the historical period. The first model
 94 is the latest available reanalysis product ERA 5 from the European Centre for Medium-Range Weather
 95 Forecasts (ECMWF) of spatial resolution ~30km x 30km (Hersbach et al., 2020). The second
 96 reanalysis model, built in the Environmental Research Laboratory (EREL) of the National Center of
 97 Scientific Research ‘Demokritos’ (NCSR-D) WRF_ERA_I, has been produced by dynamically
 98 downscaling ERA-INTERIM using the Weather Research Forecast (WRF) model (v3.6.1) from 80km
 99 x 80km to 5km x 5km (Politi et al., 2021, 2020, 2018).

100 **2.3. GCM / RCM models**

101 To observe possible alterations of WCCes occurrence probability in the future period 2025-2049
 102 compared to the historical period, we employed data from RCM simulations driven by GCMs. In this
 103 regard, we obtained data from 5 models included in the EURO-CORDEX initiative provided by the
 104 Copernicus Program. All chosen EURO-CORDEX models with available daily data for both RCP
 105 scenarios were selected because they have the finest spatial resolution of 0.11° x 0.11°, and have also
 106 been tested in Cardoso et al., (2019). Information on the regional and parent models and their acronyms
 107 used herewith is given in Table 1. In addition to the EURO-CORDEX model data, we have used
 108 dynamically downscaled data from the EC-EARTH GCM to a high spatial resolution of 5km x 5km for
 109 the area of Greece using the WRF model (Politi et al., 2020, 2022).

Μορφοποιήθηκε: Εσοχή: Αριστερά: 0 εκ.

Institution	Reference	Regional Model	Forcing model	Acronym	Resolution (°)
Météo-France / Centre National de Recherches Météorologiques	(Spiridonov et al., n.d.)	ALADIN63	CNRM-CERFACS-CNRM-CM5	CNRM	0.11
Koninklijk Nederlands Meteorologisch Instituut	(van Meijgaard et al., 2008)	KNMI-RACMO22E	ICHEC-EC-EARTH	KNMI	0.11

Climate Limited-Area Modelling Community	(Rockel et al., 2008)	CLMcom-CLM-CCLM4-8-17	MOHC-HadGEM2-ES	CLMcom	0.11
Swedish Meteorological and Hydrological Institute	(Samuelsson et al., 2016)	SMHI-RCA4	MPI-M-MPI-ESM-LR	SMHI	0.11
Danish Meteorological Institute	(Christensen, 2006)	DMI-HIRHAM5	NCC-NorESM1-M	DMI	0.11
EREL (NCSRD)	(Politi et al. 2020, 2022)	ARW-WRF	EC-EARTH	WRF_EC	0.05

110

111 **Table 1: EURO-CORDEX and EREL-NCSRD simulation models information.**

112

113 **3. Methodology**

114 The first step in this study is the validation of the projection and reanalysis models against
 115 observations. Moreover, the ensemble of the 6 projection models is also exhibited. We choose as the
 116 Ensemble resolution ~~that~~ of the CORDEX models since 5 of them share the same spatial resolution.
 117 The only model in need of regridding is WRF_EC. We follow the nearest neighbor method to upscale
 118 WRF_EC from 5 km to 11 km. In addition, we use box-plots to depict the ability of the models to
 119 simulate observational data WCCEs probabilities for the historical period at the cells that include
 120 meteorological stations. The box-plots consist of the colored box, where in the band near the middle of
 121 the box is the median, the bottom and top of each color box are the 25th (Q1) and 75th (Q3) percentiles
 122 (BL) percentile. The lower limit of the whisker (LLW) is calculated by $LW = Q1 - 1.5 * BL$ and the upper
 123 limit (ULW) by $UW = Q3 + 1.5 * BL$. The length of the whiskers (WL) is calculated as the difference
 124 between ULW and LLW. Any value out of this range is marked by a black point in the plot. The
 125 validation is conducted after the elevation bias correction of temperature at the cells of the models
 126 containing the stations. The cells of the stations are found using the nearest neighbor approach and the
 127 temperature bias correction temperature is the following:

128
$$T_s = T_m + 0.006 * (H_m - H_s) \quad (1)$$

129 In equation (1), T_s is the temperature of the cell after the elevation bias correction, T_m is the
 130 temperature provided by the model, H_m is the cell elevation and H_s is the elevation of the HNMS
 131 station.

132 **3.1. Compound event selection**

133 According to HNMS, the meteorological year can be split into two climate periods
 134 (<http://emy.gr/emy/el/climatology/climatology>). The cold and wet period extends on average from mid-
 135 October to the end of March, and the warm-dry period occurs during the rest of the year. Since the
 136 study is focused on the extreme WCCEs, we examine the period between November and April, since
 137 according to the HNMS observations, April exhibits lower temperatures than October and more rainy
 138 days. Moreover, it is not uncommon for the northern parts of Greece, and especially mountainous
 139 areas, to be affected by snowfalls during April. This leads to the creation of a timeseries of 4532 daily
 140 values for the historical period and 4531 for the future period. CLMcom considers that each month is
 141 consisted by of 30 days, thus leading to 4500 values for each period. Also, DMI considers that a
 142 calendar year has 365 days, thus each period examined has 4525 values.

143 The WCCEs, which are examined on daily basis, are divided into two types of synchronous events,
 144 TX-RR and TN-RR and studied using the fixed threshold approach (Table 2). This approach considers
 145 the fixed threshold of 20 mm/day for RR and 0 °C for TN and TX for all stations or grid points, as
 146 recommended by the Commission for Climatology (CCL), the World Climate Research Programme

Αλλαγή κωδικού πεδίου

147 (WCRP) of the Climate Variability and Predictability Component (CLIVAR) project and the Expert
 148 Team for Climate Change Detection and Indices (ETCCDI). TN equal to or under 0 °C indicates Frost
 149 Days (FD), while TX equal to or under 0 °C indicates Iced Days (ID) (Fonseca et al., 2016). The
 150 thresholds examined have been proposed in various works for studying extreme events (Raziei et al.,
 151 2014; Tošić and Unkašević, 2013; Anagnostopoulou and Tolika, 2012; Pongrácz et al., 2009;
 152 Kundzewicz et al., 2006; Moberg et al., 2006).

THRESHOLDS	RR	TN	TX	WCCE	
FIXED	>= 20 mm/day (RR20)	<= 0 °C (FD)	<= 0 °C (ID)	1. 2.	(RR20-FD) (RR20-ID)

153

154 **Table 2: Univariate thresholds and the compound events examined in the study.**

155 **3.2. WCCEs probability calculation**

156 The WCCEs probabilities are calculated by applying two different methods. The first is the empirical
 157 approach counting the events from the timeseries and dividing by the total number of days to find the
 158 percentage (%) of the occurrence probability. For the second method, we use the copula approach for
 159 the HNMS observations and model comparison and to map the differences between the two methods
 160 for the reanalysis and projection of model data. Compared to copula, an empirical method has a higher
 161 uncertainty when calculating the probability of extreme events (Hao et al., 2018; Tavakol et al., 2020;
 162 Zscheischler and Seneviratne, 2017). The purpose of using two different methods is to investigate
 163 whether the copula method underestimates or overestimates the WCCEs.

164 The best fitting copula selection for each timeseries is examined using the R programming language
 165 function BiCopSelect as suggested in (Zhou et al., 2019)(Zhou et al., 2019)(Zhou et al., 2019)(Zhou et
 166 al., 2019)(Zhou et al., 2019)(Zhou et al., 2019)(Zhou et al., 2019)(Zhou et al., 2019)(Zhou et al.,
 167 2019)(Zhou et al., 2019)(Zhou et al., 2019)(Zhou et al., 2019)(Zhou et al., 2019) package VineCopula
 168 (Schepsmeier et al., 2013). The appropriate bivariate copula for each dataset is chosen by the function,
 169 from a multitude of 40 different copula families using the Akaike Information Criterion (AIC) (Akaike,
 170 1974) and Bayesian Information Criterion (BIC) and the copula chosen for each station and model
 171 dataset is shown in Appendix B (Tables B1 and B2). Copulas are used in plenty of studies that
 172 investigate the dependence between two different climate variables and the joint probability of
 173 compound events (Tavakol et al., 2020; Dzapire et al., 2020; Pandey et al., 2018; Cong and Brady,
 174 2012; Abraj and Henaarachchi, 2021).

175 As mentioned in Nelsen, (2007), a bivariate copula is a bivariate distribution function where margins
 176 are uniform on the unit interval [0, 1]. A bivariate copula is a map $C: [0,1]^2 \rightarrow [0,1]$ with $C(u,1)=u$ and
 177 $C(1,v)=v$. Let X and Y be random variables with a joint distribution function $F(x,y)=Pr(X \leq x, Y \leq y)$ and
 178 continuous marginal distribution functions $F_1(x)=Pr(X \leq x)$ and $F_2(y)=Pr(Y \leq y)$, respectively. By Sklar's
 179 theorem (Sklar, 1959), one obtains a unique representation as follows:

180
$$F(x,y) = C\{F_1(x), F_2(y)\} \tag{2}$$

181 For the two random variables of X (e.g., precipitation) and Y (e.g., temperature) with cumulative
 182 distribution functions (CDFs) $F_1(x)=Pr(X >= x)$ and $F_2(y)=Pr(Y <= y)$, the bivariate joint distribution
 183 function or copula (C) can be written as:

184
$$F(x,y) = Pr(X >= x, Y <= y) = C(u,v) \tag{3}$$

185 **4. WCCEs assessment in HNMS stations**

186 In this section, the models are validated against observations both for the empirical and the copula
 187 method. WCCEs probabilities for each station and model are presented in the supplementary material.
 188 BIAS and RMSE along with the Critical Success Index (CSI) are used for the validation. CSI is
 189 calculated as: $CSI = A / (A + B + C)$. A, B and C symbolize elements from the contingency table (Table 2)
 190 that occur from comparing zero and non-zero probabilities in stations with the corresponding model

Μορφοποίηση: Επισήμανση
 Μορφοποίηση: Επισήμανση
 Μορφοποίηση: Επισήμανση

191 cells. Also, the total number of events calculated for both methods from observational data are is
 192 presented in for each station.

MODEL EVENT	"EVENT"=POSITIVE PROBABILITY		OBSERVATION EVENT	
	YES	NO	YES	NO
			A	B
			C	D

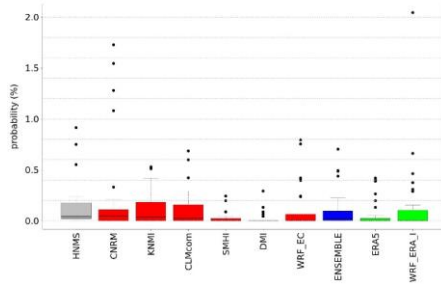
193 Table 2: Contingency table where "A" is the number of event forecasts that correspond to event
 194 observations, or the number of hits. Entry "B" is the number of event forecasts that do not
 195 correspond to observed events, or the number of false alarms. Entry "C" is the number of no-
 196 event forecasts corresponding to observed events, or the number of misses. Entry "D" is the
 197 number of no-event forecasts corresponding to no events observed, or the number of correct
 198 rejections.

199 ~~4.1~~ **4.1. RR20FD**

200 Probability values for each station are presented in Supplementary (Tables S1-S4) as well as the
 201 contingency tables (Tables S7-S10) from which CSI is calculated. ERA5 and WRF_ERA_I are
 202 reanalysis products and exhibited for comparison reasons. The copulas selected by Bicopselect for each
 203 observational and modeled timeseries are also presented in Supplementary (Tables S5-S6).

204

Μορφοποίηση: Γραμματοσειρά: (Προεπιλεγμένη) Times New Roman, 10 στ., Έντονα
Μορφοποιήθηκε: Βασικό, Χωρίς κουκκίδες ή αρίθμηση

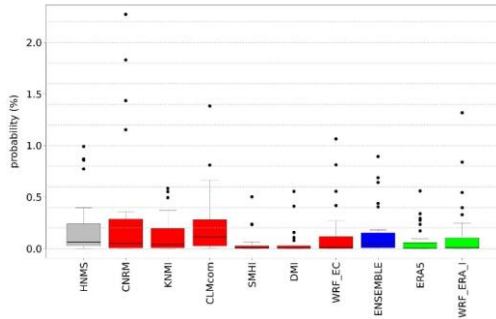


205

206 **Figure 2: Box-plot presenting RR20FD empirical method probabilities for observations and**
 207 **models.**

	<i>HNMS</i>	<i>CNRM</i>	<i>KNMI</i>	<i>CLMcom</i>	<i>SMHI</i>	<i>DMI</i>	<i>WRF_EC</i>	<i>ENSEMBLE</i>	<i>ERA5</i>	<i>WRF_ERA_I</i>
MEAN	0.1382	0.2361	0.1168	0.1116	0.0267	0.0208	0.1143	0.1044	0.0625	0.1535
SD	0.2211	0.4821	0.1590	0.1781	0.0581	0.0600	0.2216	0.1813	0.1311	0.3935
BIAS		-0.0979	0.0214	0.0266	0.1115	0.1174	0.0239	0.0338	0.0756	-0.0154
RMSE		0.3234	0.1298	0.0922	0.2003	0.2148	0.1222	0.0975	0.1536	0.2319
COR		0.8583	0.8138	0.9211	0.9194	0.7177	0.8484	0.9118	0.8210	0.8523
CSI		0.6071	0.6667	0.6296	0.3214	0.1667	0.3793	0.7692	0.2667	0.4483

208 **Table 3: Table exhibiting mean (MEAN) station RR20FD empirical probabilities (%) for**
 209 **observations and models, standard deviation (SD), bias (BIAS), rmse (RMSE), Pearson**
 210 **correlation (COR) and CSI of models against observations.**



211

212 **Figure 3: Box-plot presenting RR20FD copula method probabilities for observations and models.**

	<i>HNMS</i>	<i>CNRM</i>	<i>KNMI</i>	<i>CLMcom</i>	<i>SMHI</i>	<i>DMI</i>	<i>WRF_EC</i>	<i>ENSEMBLE</i>	<i>ERA5</i>	<i>WRF_ERA_I</i>
<i>MEAN</i>	0.2016	0.2974	0.1291	0.2129	0.0448	0.0528	0.1338	0.1451	0.0699	0.1455
<i>SD</i>	0.2864	0.5802	0.1715	0.3031	0.1042	0.1237	0.2580	0.2310	0.1368	0.2939
<i>BIAS</i>		-0.0959	0.0725	-0.0113	0.1568	0.1488	0.0678	0.0565	0.1317	0.0561
<i>RMSE</i>		0.3334	0.1720	0.2264	0.2646	0.2530	0.1458	0.1139	0.2165	0.1788
<i>COR</i>		0.9422	0.8782	0.6968	0.7688	0.7620	0.8888	0.9467	0.8955	0.8233
<i>CSI</i>		0.9259	0.9629	1	0.9643	0.7333	0.8276	1	0.6333	0.7931

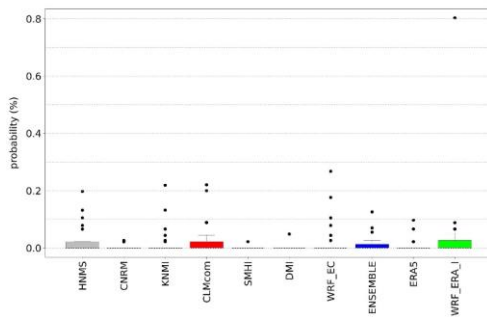
213 **Table 4: Table exhibiting mean (MEAN) RR20FD copula station probabilities (%) for**
 214 **observations and models, standard deviation (SD), bias (BIAS), rmse (RMSE), Pearson**
 215 **correlation (COR) and CSI of models against observations.**

216

217 **4.2. RR20ID**

218 RR20ID events yield, as expected, lower probabilities than RR20FD events as observed in Figures 4
 219 and 5. Most observations and models yield zero probabilities, hence validation of models for these
 220 events is limited. The empirical method exhibits eight stations with non-zero probabilities in
 221 the historical period (Supplementary).

222



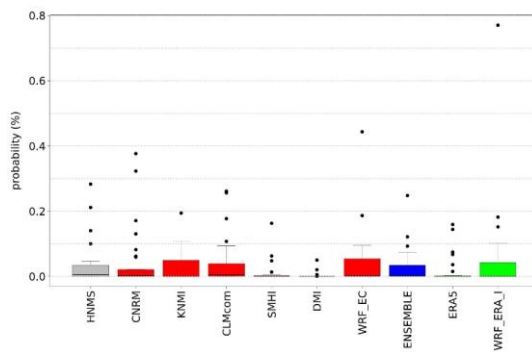
223

224 **Figure 4: Box-plot presenting RR20ID empirical method probabilities for observations and**
 225 **models.**

	<i>HNMS</i>	<i>CNRM</i>	<i>KNMI</i>	<i>CLMcom</i>	<i>SMHI</i>	<i>DMI</i>	<i>WRF_EC</i>	<i>ENSEMBLE</i>	<i>ERA5</i>	<i>WRF_ERA_I</i>
--	-------------	-------------	-------------	---------------	-------------	------------	---------------	-----------------	-------------	------------------

<i>MEAN</i>	0.0331	0.0430	0.0240	0.0397	0.0104	0.0029	0.0388	0.0265	0.0167	0.0493
<i>SD</i>	0.0669	0.0933	0.0440	0.0725	0.0320	0.0098	0.0876	0.0524	0.0413	0.1441
<i>BIAS</i>		-0.0099	0.0091	-0.0065	0.0228	0.0303	-0.0057	0.0067	0.0164	-0.0161
<i>RMSE</i>		0.0568	0.0466	0.0556	0.0522	0.0682	0.0636	0.0419	0.0438	0.1084
<i>COR</i>		0.7961	0.7212	0.6780	0.7506	0.5380	0.6829	0.7776	0.8101	0.6928
<i>CSI</i>		0.1071	0.2000	0.1923	0.0333	0.0333	0.1481	0.2400	0.1034	0.1538

226 **Table 5: Table exhibiting mean (MEAN) RR20ID empirical probabilities station probabilities**
 227 **(%) for observations and models, standard deviation (SD), bias (BIAS), rmse (RMSE), Pearson**
 228 **correlation (COR) and CSI of models against observations.**



229 **Figure 5: Box-plot presenting RR20ID copula method probabilities for observations and models.**

	<i>HNMS</i>	<i>CNRM</i>	<i>KNMI</i>	<i>CLMcom</i>	<i>SMHI</i>	<i>DMI</i>	<i>WRF_EC</i>	<i>ENSEMBLE</i>	<i>ERA5</i>	<i>WRF_ERA_I</i>
<i>MEAN</i>	0.0282	0.0378	0.0169	0.0344	0.0066	0.0017	0.0249	0.0204	0.0138	0.0274
<i>SD</i>	0.0663	0.0811	0.0303	0.0676	0.0166	0.0046	0.0473	0.0364	0.0377	0.0524
<i>BIAS</i>		-0.0097	0.0112	-0.0062	0.0215	0.0264	0.0032	0.0078	0.0144	0.0008
<i>RMSE</i>		0.0532	0.0493	0.0598	0.0565	0.0691	0.0489	0.0443	0.0420	0.0339
<i>COR</i>		0.7534	0.7228	0.5861	0.8202	0.2291	0.6594	0.7712	0.8370	0.8540
<i>CSI</i>		0.5000	0.4333	0.8095	0.5357	0.2667	0.5000	0.8095	0.2667	0.4286

231 **Table 6: Table exhibiting mean (MEAN) RR20ID copula probabilities station probabilities (%)**
 232 **for observations and models, standard deviation (SD), bias (BIAS), rmse (RMSE), Pearson**
 233 **correlation (COR) and CSI of models against observations.**

234 **4.3. Observations-models comparison conclusions**

Μορφοποίηση: Γραμματοσειρά: Έντονα

235 The events examined are rare among the available stations for the historical period. Copulas
 236 considering the dependence between the variables yield greater probabilities than the empirical method.
 237 More stations with non-zero probabilities enable more accurate validation of the models. To minimize
 238 uncertainties, smooth extreme underestimations or overestimations of WCCE probabilities that each
 239 model yields, and because ENSEMBLE shows better consistency among the projection models'
 240 statistical indices, we use it for further analysis in the study.

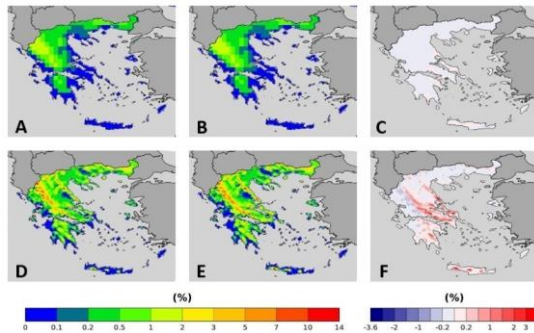
241 **5. Historical period models WCCEs on maps**

242 In this section, WCCEs spatial distribution probabilities are compared between empirical and copula
 243 methods. This procedure is conducted separately for the two reanalysis products and the Ensemble
 244 mean of the projection models.

245 **5.1. Reanalysis**

246 ERA5 and WRF_ERA_I WCCEs spatial distribution probabilities in Greece are displayed in this
 247 section. We display both reanalysis products, although ERA5 is the most recently developed reanalysis
 248 product, we exhibit also WRF_ERA_I since its much finer spatial resolution is more appropriate for the
 249 complex topography of Greece with many mountains and islands.

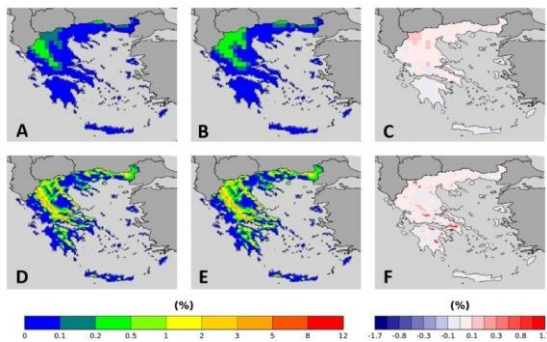
250



251

252 **Figure 6: RR20FD probabilities for (A, B, C) ERA5 and (D, E, F) WRF_ERA_I produced by (A,**
 253 **D) Empirical and (B, E) Copula and (C) = (B) –(A) and (F)=(E)-(D).**

254



255

256 **Figure 7: RR20ID probabilities for (A, B, C) ERA5 and (D, E, F) WRF_ERA_I produced by**
 257 **(A,D) Empirical and (B, E) Copula and (C) = (B)–(A) and (F) = (E)-(D).**

258 Both reanalysis products yield greater WCCEs probabilities in the Pindus mountains, although due to
 259 its finer spatial resolution, WRF_ERA_I display high probabilities at other mountainous regions
 260 located in Crete, Peloponnese, Evia Island and others. Also, in both WCCEs copula method yields
 261 higher probabilities, especially for WRF_ERA_I and the RR20FD case. Moreover, WRF_ERA_I
 262 displays a greater range than ERA5 with RR20FD probabilities reaching 14% and RR20ID 12%
 263 compared to 6% and 2% of ERA5 respectively.

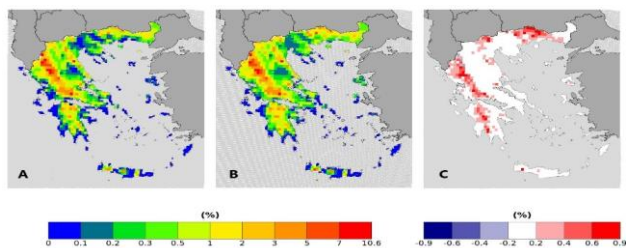
264 **6.2.5.2 Projections Ensemble**

265 Figures 8 and 9 yield that the Ensemble mean displays similar to the WRF_ERA_I spatial distributions
 266 of WCCEs. RR20FD and RR20ID probabilities reach 10.8% and 5.4% respectively. The copula
 267 method yields higher probabilities for both methods in mountainous regions with greater differences

Μορφοποίηση: Γραμματοσειρά: (Προεπιλεγμένη) Times New Roman, 10 στ., Έντονα
Μορφοποιήθηκε: Παράγραφος λίστας, Αριθμημένη διάρθρωση + Επίπεδο: 2 + Στυλ αρίθμησης: 1, 2, 3, ... + Έναρξη από: 2 + Στοιχίση: Αριστερά + Στοιχίση: 0 εκ. + Εσοχή: 0,63 εκ.

268 displayed for RR20ID events in the Pindos mountain range and RR20FD exhibiting greater spatial
 269 distribution in differences between the two methods.

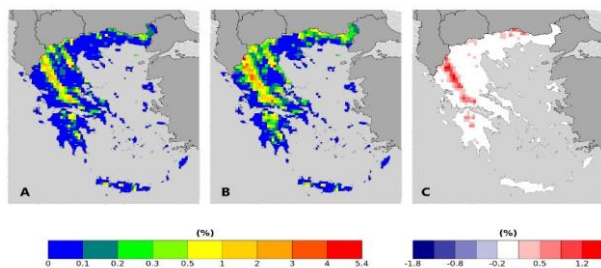
270



271

272 **Figure 8: RR20FD Ensemble probabilities for (A) Empirical and (B) Copula method. (C)=(B)-**
 273 **(A).**

274



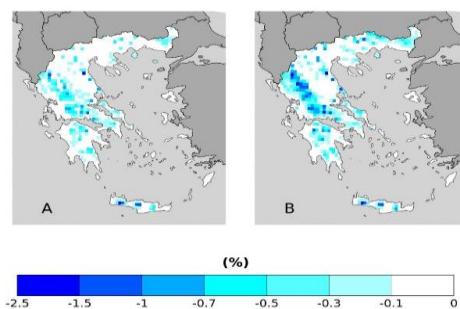
275

276 **Figure 9: RR20ID Ensemble probabilities for (A) Empirical and (B) Copula method. (C)=(B)-(A).**

277 **6. Past-Future Ensemble differences**

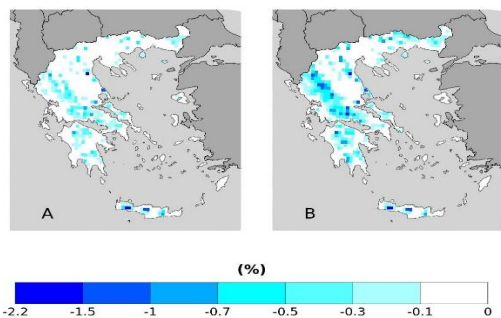
278 This section displays the differences of the Ensemble mean WCCEs probabilities, calculated for the
 279 empirical and the copula method, compared to the past probabilities presented in the previous section.
 280 The differences mapped are statistically significant at a 95% level using the Student's t-test (Goulden,
 281 1939) comparing 25 annual values of the timeseries.

282 **6.1 RR20FD**



283

284 Figure 10: RR20FD empirical method probability differences of future-past periods for (A)
 285 RCP4.5 and (B) RCP8.5 scenarios.



286

287 Figure 11: RR20FD copula method probability differences of future-past periods for (A) RCP4.5
 288 and (B) RCP8.5 scenarios.

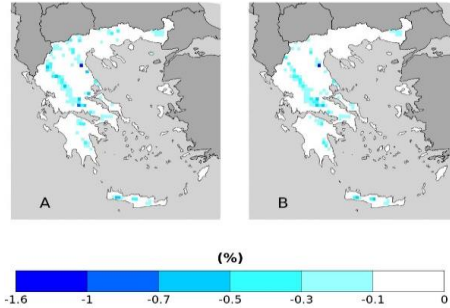
	<i>Empirical RCP4.5</i>	<i>Empirical RCP8.5</i>	<i>Copula RCP4.5</i>	<i>Copula RCP8.5</i>
$0 \leq Nc < 0.1$	34	31	64	57
$-0.1 \leq Nc < 0.3$	112	154	112	131
$-0.3 \leq Nc < 0.5$	63	65	53	81
$-0.5 \leq Nc < 0.7$	31	48	16	47
$-0.7 \leq Nc < 1$	12	34	6	24
$-1 \leq Nc < 1.5$	5	18	3	11
$Nc \leq -1.5$	2	5	3	4
<i>MAX D</i>	-1.8063 %	-2.4988 %	-1.9500 %	-2.1392 %

289 Table 7: ENSEMBLE Number of cells (Nc) in each category of probability difference (%) for
 290 RR20FD for empirical and copula method. MAX D denotes the maximum negative difference
 291 between future and past periods. Nv concerns only cells with statistically significant difference.

292 From the results displayed in Figures 10 and 11 and in Table 7 RCP4.5 and RCP8.5 scenarios for the
 293 probabilities of the RR20FD events, we observe that in all cases future scenarios yield only negative
 294 values, meaning the reduction of RR20FD events in the 2025-2049 period compared to 1980-2004
 295 period in all mountainous regions of Greece. RCP8.5 yields a greater reduction of RR20FD
 296 probabilities than the RCP4.5 scenario both in spatial distribution and extreme values. The empirical
 297 method exhibits a greater reduction for the RCP8.5 scenario, although for the RCP4.5 scenario both
 298 methods yield similar results.

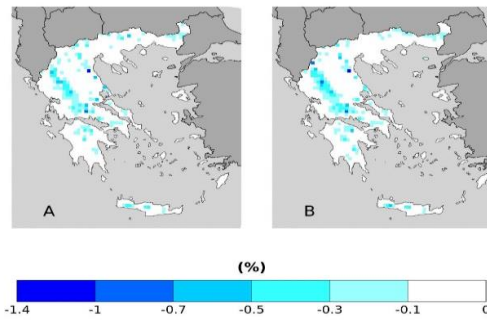
299 **6.2 6.2. RR20ID**

Μορφοποιήθηκε: Χωρίς κουκκίδες ή αρίθμηση



300

301 **Figure 12: RR20ID empirical method probability differences of future-past periods for (A)**
 302 **RCP4.5 and (B) RCP8.5 scenarios.**



303

304 **Figure 13: RR20ID copula method probability differences of future-past periods for (A) RCP4.5**
 305 **and (B) RCP8.5 scenarios.**

	<i>Empirical RCP4.5</i>	<i>Empirical RCP8.5</i>	<i>Copula RCP4.5</i>	<i>Copula RCP8.5</i>
$0 \leq Nc < 0.1$	193	229	166	210
$-0.1 \leq Nc < -0.3$	81	71	96	109
$-0.3 \leq Nc < -0.5$	23	20	33	37
$-0.5 \leq Nc < -0.7$	9	5	9	7
$-0.7 \leq Nc < -1$	1	0	1	3
$Nc \leq -1$	1	1	1	1
<i>MAX D</i>	-1.5536	-1.0593	-1.3425	-1.1362

306 **Table 8: ENSEMBLE Number of cells (Nc) in each category of probability difference (%) for**
 307 **RR20ID for empirical and copula method. MAX D denotes the maximum negative difference**
 308 **between future and past periods. Nv concerns only cells with statistically significant difference.**

309 Similarly, to RR20FD, RR20ID events probabilities yield only zero or negative differences compared
 310 to the past for both scenarios. Empirical and copula methods yield similar results in distribution and
 311 extreme values. For both methods, the RCP4.5 scenario tends to higher reduction of RR20ID
 312 probabilities than RCP8.5, as observed in Table 8.

313 The results for both scenarios and events show that independently from the choice of scenario, the
 314 probabilities of the events are expected to reduce almost equally in the near future (2025-2049)
 315 compared to the past period (1980-2004).

316 7. Discussion and Conclusions

317 This work presents for the first time to our knowledge an extensive study of wet-cold compound events
318 in Greece for the historical and future periods of 1980-2004 and 2025-2049, respectively. Models' data
319 from the EUROCORDEX initiative of 0.11° resolution and reanalysis data (ERA5 and ERA-Interim
320 dynamically downscaled to 5km²) were used and validated for the determined WCCEs against the
321 formally available observational datasets by HNMS for the country. The number of events and their
322 probabilities of occurrence were determined by applying a fixed thresholds approach. Then, the
323 bivariate validation of the models' datasets against observations was performed for the determined
324 bivariate thresholds. The probabilities of WCCEs were computed using the empirical method and the
325 best-fitted copula for the bivariate timeseries for observational data, reanalysis, projection models and
326 the Ensemble of the projection models. Copulas yield higher extreme events probabilities for most of
327 the cases considering the dependence between temperature and precipitation.

328 Although, uncertainties may rise on the impact of WCCEs on mountainous areas due to the absence of
329 observations on altitudes higher than 1000 meters, we trust the results yielded by the Ensemble.
330 Besides the satisfying results from the bivariate validation, this trust is enhanced by the fact that winter
331 period systems affect large areas crossing the country from north to south or from west to east (Cartalis
332 et al., 2010) and therefore recorded by available stations. Also, in the cold period of the year,
333 convective precipitation forced by orography is limited hence the doubt that the models do not simulate
334 extreme rainfall in winter is reduced. Moreover, the use of the Ensemble mean of the models reduces
335 the uncertainties on ~~in~~ models' ability to simulate the probability of ~~the~~ occurrence of extreme events
336 ~~occurrences~~. The reduction of RR20-FD and RR20-ID WCCEs on mountains that the Ensemble of
337 projection models predict in the future, might contribute to less heavy snowfall events and possibly less
338 accumulated snow depth. If such a scenario will be verified, Greece faces the threat of losing the main
339 sources of fresh water that come from melted mountain snow during spring or early summer in the near
340 future period. The rise of temperature due to global warming is the main factor for the reduction of
341 WCCEs (Supplementary Figures S5-S7), while also possible changes in patterns of teleconnections
342 may affect winter conditions in Greek mountains, similar to NAO (North Atlantic Oscillation) pattern
343 affecting Pindos mountains (López-Moreno et al., 2011) or the positive phase of EAWR (East Atlantic-
344 Western Russia) pattern that leads to cold air advection from the north towards the southern part of
345 Europe and ~~the~~ eastern Mediterranean region (Ionita, 2014). Still, understanding ~~of~~ extreme events on
346 complex terrains demands greater effort from the scientific community to enable solid predictions on
347 the impact of climate change on the occurrence of these events.

348 Acknowledgments

349 The authors acknowledge partial funding by the project "National Research Network for Climate
350 Change and its Impacts, (CLIMPACT - 105658/17-10-2019)" of the Ministry of Development, GSRT,
351 Program of Public Investment, 2019.

352 References

- 353 Abdi, H.: The Kendall Rank Correlation Coefficient, 2007.
- 354 Abraj, M. A. M. and Hewarachchi, A. P.: Joint return period estimation of daily maximum and
355 minimum temperatures using copula method, 66, 175–190, <https://doi.org/10.17654/AS066020175>,
356 2021.
- 357 Aghakouchak, A., Chiang, F., Huning, L. S., Love, C. A., Mallakpour, I., Mazdiyasn, O., Moftakhari,
358 H., Papalexioiu, S. M., Ragno, E., and Sadegh, M.: Climate Extremes and Compound Hazards in a
359 Warming World, 48, 519–548, <https://doi.org/10.1146/ANNUREV-EARTH-071719-055228>, 2020.
- 360 Akaike, H.: A New Look at the Statistical Model Identification, 19, 716–723,
361 <https://doi.org/10.1109/TAC.1974.1100705>, 1974.
- 362 Ali, E., Cramer, W., Carnicer, J., Georgopoulou, E., Hilmi, N. J. M., le Cozannet, G., Lionello, P.,
363 Pörtner, H.-O., Roberts, D. C., Tignor, M., Poloczanska, E. S., Mintenbeck, K., Alegria, A., Craig, M.,

364 Langsdorf, S., Löschke, S., Möller, V., Okem, A., and Rama, B.: SPM 2233 CCP4 Mediterranean
365 Region to the Sixth Assessment Report of the Intergovernmental Panel on Climate Change [2233–
366 2272, <https://doi.org/10.1017/9781009325844.021>, n.d.

367

368 Anagnostopoulou, C. and Tolika, K.: Extreme precipitation in Europe: Statistical threshold selection
369 based on climatological criteria, 107, 479–489, [https://doi.org/10.1007/S00704-011-0487-
370 8/TABLES/2](https://doi.org/10.1007/S00704-011-0487-8/TABLES/2), 2012.

371 Balkema, A. A. and Haan, L. de: Residual Life Time at Great Age, 2, 792–804,
372 <https://doi.org/10.1214/AOP/1176996548>, 1974.

373 Cartalis, C., Chrysoulakis, N., Feidas, H., and Pitsitakis, N.: International Journal of Remote Sensing
374 Categorization of cold period weather types in Greece on the basis of the photointerpretation of
375 NOAA/AVHRR imagery Categorization of cold period weather types in Greece on the basis of the
376 photointerpretation of NOAA/AVHRR imagery, <https://doi.org/10.1080/01431160310001632684>,
377 2010.

378 Cardoso, R. M., Soares, P. M. M., Lima, D. C. A., and Miranda, P. M. A.: Mean and extreme
379 temperatures in a warming climate: EURO CORDEX and WRF regional climate high-resolution
380 projections for Portugal, 52, 129–157, <https://doi.org/10.1007/S00382-018-4124-4/FIGURES/8>, 2019.

381 Christensen, O. B.: Regional climate change in Denmark according to a global 2-degree-warming
382 scenario, 2006.

383 Chukwudum, Q. C. and Nadarajah, S.: Bivariate Extreme Value Analysis of Rainfall and Temperature
384 in Nigeria, *Environmental Modeling and Assessment*, 27, 343–362, [https://doi.org/10.1007/S10666-
385 021-09781-7/TABLES/13](https://doi.org/10.1007/S10666-021-09781-7/TABLES/13), 2022.

386 Coles, S.: An Introduction to Statistical Modeling of Extreme Values, [https://doi.org/10.1007/978-1-
387 4471-3675-0](https://doi.org/10.1007/978-1-4471-3675-0), 2001.

388 Cong, R. G. and Brady, M.: The interdependence between rainfall and temperature: Copula analyses,
389 2012, <https://doi.org/10.1100/2012/405675>, 2012.

390 Curtis, S., Fair, A., Wistow, J., Val, D. v., and Oven, K.: Impact of extreme weather events and climate
391 change for health and social care systems, 16, 23–32, [https://doi.org/10.1186/S12940-017-0324-
392 3/METRICS](https://doi.org/10.1186/S12940-017-0324-3/METRICS), 2017.

393 de Luca, P., Messori, G., Faranda, D., Ward, P. J., and Coumou, D.: Compound warm-dry and cold-wet
394 events over the Mediterranean, 11, 793–805, <https://doi.org/10.5194/ESD-11-793-2020>, 2020.

395 Demiroglu, O. C., Kučerová, J., and Ozcelebi, O.: Snow reliability and climate elasticity: Case of a
396 Slovak ski resort, 70, 1–12, <https://doi.org/10.1108/TR-01-2014-0003/FULL/PDF>, 2015.

397 Dzapire, N. C., Ngare, P., and Odongo, L.: A copula based bi-variate model for temperature and
398 rainfall processes, 8, e00365, <https://doi.org/10.1016/J.SCIAF.2020.E00365>, 2020.

399 Fisher, R. A. and Tippett, L. H. C.: Limiting forms of the frequency distribution of the largest or
400 smallest member of a sample, 24, 180–190, <https://doi.org/10.1017/S0305004100015681>, 1928.

401 Fonseca, D., Carvalho, M. J., Marta-Almeida, M., Melo-Gonçalves, P., and Rocha, A.: Recent trends of
402 extreme temperature indices for the Iberian Peninsula, 94, 66–76,
403 <https://doi.org/10.1016/J.PCE.2015.12.005>, 2016.

404 García-Ruiz, J. M., López-Moreno, I. I., Vicente-Serrano, S. M., Lasanta-Martínez, T., and Beguería,
405 S.: Mediterranean water resources in a global change scenario, 105, 121–139,
406 <https://doi.org/10.1016/J.EARSCIREV.2011.01.006>, 2011.

407 Gilleland, E. and Katz, R. W.: extRemes 2.0: An Extreme Value Analysis Package in R, 72, 1–39,
408 <https://doi.org/10.18637/JSS.V072.I08>, 2016.

409 Gnedenko, B.: Sur La Distribution Limite Du Terme Maximum D'Une Serie Aleatoire, 44, 423,
410 <https://doi.org/10.2307/1968974>, 1943.

411 Goda, Y.: Inherent Negative Bias of Quantile Estimates of Annual Maximum Data Due to Sample Size
412 Effect: A Numerical Simulation Study, 53, 397–429, <https://doi.org/10.1142/S0578563411002409>,
413 2018.

414 Goulden, C.: *Methods of statistical analysis.*, 1939.

415 Hao, Z., Singh, V. P., and Hao, F.: Compound Extremes in Hydroclimatology: A Review, 10, 718,
416 <https://doi.org/10.3390/W10060718>, 2018.

417 Hersbach, H., Bell, B., Berrisford, P., Hirahara, S., Horányi, A., Muñoz-Sabater, J., Nicolas, J., Peubey,
418 C., Radu, R., Schepers, D., Simmons, A., Soci, C., Abdalla, S., Abellan, X., Balsamo, G., Bechtold, P.,
419 Biavati, G., Bidlot, J., Bonavita, M., de Chiara, G., Dahlgren, P., Dee, D., Diamantakis, M., Dragani,
420 R., Flemming, J., Forbes, R., Fuentes, M., Geer, A., Haimberger, L., Healy, S., Hogan, R. J., Hólm, E.,
421 Janisková, M., Keeley, S., Laloyaux, P., Lopez, P., Lupu, C., Radnoti, G., de Rosnay, P., Rozum, I.,
422 Vamborg, F., Villaume, S., and Thépaut, J. N.: The ERA5 global reanalysis, 146, 1999–2049,
423 <https://doi.org/10.1002/QJ.3803>, 2020.

424 Hochman, A., Marra, F., Messori, G., Pinto, J., Raveh-Rubin, S., Yosef, Y., and Zittis, G.: ESD
425 Reviews: Extreme Weather and Societal Impacts in the Eastern Mediterranean, 1–53,
426 <https://doi.org/10.5194/ESD-2021-55>, 2021.

427 Houston, T. G., Changnon, S. A., Ae, T. G. H., and Changnon, S. A.: Freezing rain events: a major
428 weather hazard in the conterminous US, 40, 485–494, <https://doi.org/10.1007/S11069-006-9006-0>,
429 2006.

430 Ionita, M.: The Impact of the East Atlantic/Western Russia Pattern on the Hydroclimatology of Europe
431 from Mid-Winter to Late Spring, *Climate 2014*, Vol. 2, Pages 296-309, 2, 296–309,
432 <https://doi.org/10.3390/CLI2040296>, 2014.

433 James Pickands: Statistical Inference Using Extreme Order Statistics, 3, 119–131,
434 <https://doi.org/10.1214/AOS/1176343003>, 1975.

435 Konisky, D. M., Hughes, L., and Kaylor, C. H.: Extreme weather events and climate change concern,
436 134, 533–547, <https://doi.org/10.1007/S10584-015-1555-3/FIGURES/3>, 2016.

437 Kundzewicz, Z. W., Radziejewski, M., and Pińskwar, I.: Precipitation extremes in the changing climate
438 of Europe, 31, 51–58, <https://doi.org/10.3354/CR031051>, 2006.

439 Lazoglou, G. and Anagnostopoulou, C.: Joint distribution of temperature and precipitation in the
440 Mediterranean, using the Copula method, 135, 1399–1411, <https://doi.org/10.1007/S00704-018-2447-Z/FIGURES/5>, 2019.

442 Lemus-Canovas, M.: Changes in compound monthly precipitation and temperature extremes and their
443 relationship with teleconnection patterns in the Mediterranean, *Journal of Hydrology*, 608, 127580,
444 <https://doi.org/10.1016/J.JHYDROL.2022.127580>, 2022.

445 Leonard, M., Westra, S., Phatak, A., Lambert, M., van den Hurk, B., McInnes, K., Risbey, J., Schuster,
446 S., Jakob, D., and Stafford-Smith, M.: A compound event framework for understanding extreme
447 impacts, 5, 113–128, <https://doi.org/10.1002/WCC.252>, 2014.

448 Lhotka, O. and Kysely, J.: Precipitation–temperature relationships over Europe in CORDEX regional
449 climate models, *International Journal of Climatology*, <https://doi.org/10.1002/JOC.7508>, 2021.

450 Llasat, M. C., Turco, M., Quintana-Seguí, P., and Llasat-Botija, M.: The snow storm of 8 March 2010
451 in Catalonia (Spain): a paradigmatic wet-snow event with a high societal impact, 14, 427–441,
452 <https://doi.org/10.5194/NHESS-14-427-2014>, 2014.

453 López-Moreno, J. I., Vicente-Serrano, S. M., Morán-Tejeda, E., Lorenzo-Lacruz, J., Kenawy, A., and
454 Beniston, M.: Effects of the North Atlantic Oscillation (NAO) on combined temperature and
455 precipitation winter modes in the Mediterranean mountains: Observed relationships and projections for
456 the 21st century, *Glob Planet Change*, 77, 62–76,
457 <https://doi.org/10.1016/J.GLOPLACHA.2011.03.003>, 2011.

458 Markantonis, I., Vlachogiannis, D., Sfetsos, T., Kioutsioukis, I., and Politi, N.: An Investigation of
459 cold-wet Compound Events in Greece, <https://doi.org/10.5194/EMS2021-188>, 2021.

460 Moalafhi, D. B., Evans, J. P., and Sharma, A.: Evaluating global reanalysis datasets for provision of
461 boundary conditions in regional climate modelling, 47, 2727–2745, <https://doi.org/10.1007/S00382-016-2994-X/TABLES/9>, 2016.

463 Moberg, A., Jones, P. D., Lister, D., Walther, A., Brunet, M., Jacobeit, J., Alexander, L. v., Della-
464 Marta, P. M., Luterbacher, J., Yiou, P., Chen, D., Tank, A. M. G. K., Saladié, O., Sigró, J., Aguilar, E.,
465 Alexandersson, H., Almarza, C., Auer, I., Barriendos, M., Begert, M., Bergström, H., Böhm, R., Butler,
466 C. J., Caesar, J., Drebs, A., Founda, D., Gerstengarbe, F. W., Micela, G., Maugeri, M., Österle, H.,
467 Pandzic, K., Petrakis, M., Srnec, L., Tolasz, R., Tuomenvirta, H., Werner, P. C., Linderholm, H.,
468 Philipp, A., Wanner, H., and Xoplaki, E.: Indices for daily temperature and precipitation extremes in
469 Europe analyzed for the period 1901–2000, 111, 22106, <https://doi.org/10.1029/2006JD007103>, 2006.

470 Nelsen, R.: *An introduction to copulas*, 2007.

471 Pandey, P. K., Das, L., Jhajharia, D., and Pandey, V.: Modelling of interdependence between rainfall
472 and temperature using copula, 4, 867–879, <https://doi.org/10.1007/S40808-018-0454-9>, 2018.

473 Pestereva, N. M., Popova, N. Yu., and Shagarov, L. M.: *Modern Climate Change and Mountain Skiing
474 Tourism: the Alps and the Caucasus, 1602–1617*, 2012.

475 Politi, N., Nastos, P. T., Sfetsos, A., Vlachogiannis, D., and Dalezios, N. R.: Evaluation of the AWR-
476 WRF model configuration at high resolution over the domain of Greece, 208, 229–245,
477 <https://doi.org/10.1016/J.ATMOSRES.2017.10.019>, 2018.

478 Politi, N., Sfetsos, A., Vlachogiannis, D., Nastos, P. T., and Karozis, S.: A Sensitivity Study of High-
479 Resolution Climate Simulations for Greece, 8, 44, <https://doi.org/10.3390/CLI8030044>, 2020.

480 Politi, N., Vlachogiannis, D., Sfetsos, A., and Nastos, P. T.: High-resolution dynamical downscaling of
481 ERA-Interim temperature and precipitation using WRF model for Greece, 57, 799–825,
482 <https://doi.org/10.1007/S00382-021-05741-9/FIGURES/17>, 2021.

483 Politi, N., Vlachogiannis, D., Sfetsos, A., Nastos, P.T., High resolution projections for extreme
484 temperatures and precipitation over Greece, under review, <https://doi.org/10.21203/rs.3.rs-1263740/v1>,
485 2022

486 Pongrácz, R., Bartholy, J., Gelybó, G., and Szabó, P.: Detected and expected trends of extreme climate
487 indices for the carpathian basin, 15–28, https://doi.org/10.1007/978-1-4020-8876-6_2, 2009.

488 Razei, T., Daryabari, J., Bordi, I., Modarres, R., and Pereira, L. S.: Spatial patterns and temporal trends
489 of daily precipitation indices in Iran, 124, 239–253, [https://doi.org/10.1007/S10584-014-1096-](https://doi.org/10.1007/S10584-014-1096-1/TABLES/1)
490 [1/TABLES/1](https://doi.org/10.1007/S10584-014-1096-1/TABLES/1), 2014.

491 Rockel, B., Will, A., and Hense, A.: The regional climate model COSMO-CLM (CCLM), 17, 347–348,
492 <https://doi.org/10.1127/0941-2948/2008/0309>, 2008.

493 Sadegh, M., Moftakhari, H., Gupta, H. v., Ragno, E., Mazdiyasi, O., Sanders, B., Matthew, R., and
494 AghaKouchak, A.: Multihazard Scenarios for Analysis of Compound Extreme Events, 45, 5470–5480,
495 <https://doi.org/10.1029/2018GL077317>, 2018.

496 Samuelsson, P., Jones, C. G., Willén, U., Ullerstig, A., Gollvik, S., Hansson, U., Jansson, C.,
497 Kjellström, E., Nikulin, G., and Wyser, K.: The Rossby Centre Regional Climate model RCA3: model
498 description and performance, 63, 4–23, <https://doi.org/10.1111/J.1600-0870.2010.00478.X>, 2016.

499 Schepsmeier, U., Stoeber, J., Christian, E., and Maintainer, B.: Package “VineCopula” Type Package
500 Title Statistical inference of vine copulas, 2013.

501 Schwarz, G.: Estimating the Dimension of a Model, <https://doi.org/10.1214/aos/1176344136>, 6, 461–
502 464, <https://doi.org/10.1214/AOS/1176344136>, 1978.

503 Singh, H., Najafi, M. R., and Cannon, A. J.: Characterizing non-stationary compound extreme events in
504 a changing climate based on large-ensemble climate simulations, 56, 1389–1405,
505 <https://doi.org/10.1007/S00382-020-05538-2/FIGURES/6>, 2021.

506 Sklar and M.: Fonctions de repartition a n dimensions et leurs marges, 8, 229–231, 1959.

507 Spiridonov, V., Somot, S., and Déqué, M.: ALADIN-Climate: from the origins to present date, n.d.

508 Tavakol, A., Rahmani, V., and Harrington, J.: Probability of compound climate extremes in a changing
509 climate: A copula-based study of hot, dry, and windy events in the central United States, 15, 104058,
510 <https://doi.org/10.1088/1748-9326/ABB1EF>, 2020.

511 Tošić, I. and Unkašević, M.: Extreme daily precipitation in Belgrade and their links with the prevailing
512 directions of the air trajectories, 111, 97–107, <https://doi.org/10.1007/S00704-012-0647-5/FIGURES/9>,
513 2013.

514 Tringa E and Kostopoulou E: An observational study of the relationships between extreme temperature
515 and precipitation and the surface atmospheric circulation in Greece, n.d.

516 Trujillo, E., Molotch, N. P., Goulden, M. L., Kelly, A. E., and Bales, R. C.: Elevation-dependent
517 influence of snow accumulation on forest greening, 5, 705–709, <https://doi.org/10.1038/ngeo1571>,
518 2012.

519 Vajda, A., Tuomenvirta, H., Juga, I., Nurmi, P., Jokinen, P., and Rauhala, J.: Severe weather affecting
520 European transport systems: The identification, classification and frequencies of events, 72, 169–188,
521 <https://doi.org/10.1007/S11069-013-0895-4/TABLES/3>, 2014.

522 van Meijgaard, E., van Ulft, L. H., van de Berg, W. J., Bosveld, F. C., van den Hurk, B. J. J. M.,
523 Lenderink, G., and Siebesma, A. P.: The KNMI regional atmospheric climate model RACMO version
524 2.1, 2008.

525 Vogel, J., Paton, E., and Aich, V.: Seasonal ecosystem vulnerability to climatic anomalies in the
526 Mediterranean, 18, 5903–5927, <https://doi.org/10.5194/BG-18-5903-2021>, 2021.

527 Voudouri, A. and Kotta, D.: Factors Determined Snow Accumulation Over the Greater Athens Area
528 During the Latest Snowfall Events, 355–361, https://doi.org/10.1007/978-3-642-29172-2_50, 2013.

529 Wu, X., Hao, Z., Hao, F., and Zhang, X.: Variations of compound precipitation and temperature
530 extremes in China during 1961–2014, *Science of The Total Environment*, 663, 731–737,
531 <https://doi.org/10.1016/J.SCITOTENV.2019.01.366>, 2019.

532 Zanicco, C., Boudet, H., Nilson, R., Satein, H., Whitley, H., and Flora, J.: Place, proximity, and
533 perceived harm: extreme weather events and views about climate change, 149, 349–365,
534 <https://doi.org/10.1007/S10584-018-2251-X/TABLES/2>, 2018.

535 Zhang, W., Luo, M., Gao, S., Chen, W., Hari, V., and Khouakhi, A.: Compound Hydrometeorological
536 Extremes: Drivers, Mechanisms and Methods, 9, 941,
537 <https://doi.org/10.3389/FEART.2021.673495/BIBTEX>, 2021.

538 Zscheischler, J. and Seneviratne, S. I.: Dependence of drivers affects risks associated with compound
539 events, 3, https://doi.org/10.1126/SCIADV.1700263/SUPPL_FILE/1700263_SM.PDF, 2017.

540 Zscheischler, J., Orth, R., and Seneviratne, S. I.: Bivariate return periods of temperature and
541 precipitation explain a large fraction of European crop yields, 14, 3309–3320,
542 <https://doi.org/10.5194/BG-14-3309-2017>, 2017.

543 Zscheischler, J., Westra, S., van den Hurk, B. J. J. M., Seneviratne, S. I., Ward, P. J., Pitman, A.,
544 AghaKouchak, A., Bresch, D. N., Leonard, M., Wahl, T., and Zhang, X.: Future climate risk from
545 compound events, 8, 469–477, <https://doi.org/10.1038/s41558-018-0156-3>, 2018.

546 Zhou, S., Zhang, Y., Williams, A. P., and Gentine, P.: Projected increases in intensity, frequency, and
547 terrestrial carbon costs of compound drought and aridity events, *Science Advances*, 5,
548 https://doi.org/10.1126/SCIADV.AAU5740/SUPPL_FILE/AAU5740_SM.PDF, 2019.

549 **Code and data availability**

550 Code and results data available upon request.

551 **Author contributions**

552 IM has worked on conceptualization, methodology, validation, visualization, investigation, writing
553 review and editing. AS, DV and IK contributed on conceptualization, review and supervision. All
554 authors have read and agreed to the published version of the manuscript.

555 **Competing interests**

556 The authors declare that they have no conflict of interest.

557

558 **Appendix**

NUMBER	LOCATION	ID	LATITUDE	LONGITUDE	ELEVATION (m)	YEARS
1	Alexandroupoli	16627	40.85	25.917	4	1980-2004
2	Elliniko	16716	37.8877	23.7333	10	1980-2004
3	Ioannina	16642	39.7	20.817	483	1980-2004
4	Irakleio	16754	35.339	25.174	39	1980-2004
5	Kalamata	16726	37.067	22.017	6	1980-2004

6	Kastoria	16614	40.45	21.28	660.95	1980-2004
7	Kerkira	16641	39.603	19.912	1	1980-2004
8	Kithira	16743	36.2833	23.0167	167	1980-2004
9	Larisa	16648	39.65	22.417	73	1980-2004
10	Limnos	16650	39.9167	25.2333	4	1980-2004
11	Methoni	16734	36.8333	21.7	34	1980-2004
12	Milos	16738	36.7167	24.45	183	1980-2004
13	Mitilini	16667	39.059	26.596	4	1980-2004
14	Naxos	16732	37.1	25.383	9	1980-2004
15	Rhodes	16749	36.42896	28.21661	95	1980-2004
16	Samos	16723	37.79368	26.68199	10	1980-2004
17	Skyros	16684	38.9676	24.4872	12	1980-2004
18	Souda	16746	35.4833	24.1167	151	1980-2004
19	Thessaloniki	16622	40.517	22.967	2	1980-2004
20	Tripoli	16710	37.527	22.401	651	1980-2004
21	Zakinthos	16719	37.751	20.887	5	1980-2004
22	Florina	16613	40.78	21.43	619	1980-2002
23	Aktio	16643	38.919	20.772	2	1980-2004
24	Anchialos	16665	39.217	22.8	19	1980-2000
25	Lamia	16675	38.883	22.433	12	1980-2004
26	Andravida	16682	37.92	21.293	10	1980-2004
27	Patras	16689	38.25	21.733	2	1980-1999
28	Tanagra	16699	38.317	23.533	140	1980-2000
29	Chios	16706	38.333	26.133	5	1980-2000
30	Elefsis	16718	38.064	23.556	20	1980-2000

559

560 **Table A1: HNMS stations information.**

561

562

563

564

565